Available online at www.sciencedirect.com
SCIENCE DIRECT

Infrared Physics & Technology 48 (2006) 217–222

INFRARED PHYSICS & TECHNOLOGY

www.elsevier.com/locate/infrared

Frictionless mirror drive for intermediate resolution infrared Fourier transform spectroscopy

G. Bianchini, F. Castagnoli, M. Pellegrini, L. Palchetti *

Istituto di Fisica Applicata ''Nello Carrara'' CNR-IFAC, Via Panciatichi, 64, 50127 Florence, Italy

Received 24 June 2005
Available online 14 November 2005

Abstract

A simple and compact parallelogram mirror drive based on flexure pivots suitable for intermediate resolution Fourier transform spectroscopy is presented. The system permits 12 mm of mirror translation with a residual tilt of less than ±0.4 mrad in the horizontal plane and ±0.2 mrad in the vertical plane. A system prototype was built and fully characterized for a Fourier transform spectrometer operating on a stratospheric balloon.

PACS: 33.20.Ea; 93.85.+q; 07.87.+v

Keywords: Fourier transform spectroscopy; Mirror drive

1. Introduction

A common problem in Fourier transform spectrometers (FTS) is the design of an effective mirror drive compliant with the alignment requirements particularly in the case of the long path differences needed in a high-resolution instrument. This is a major problem in the case of instrumentation designed to operate from aerospatial platforms, where after the shocks and vibrations of the launch, long term unattended operation is needed.

Mirror drive quality directly affects the data in terms of phase and sampling errors resulting in data degradation or, at least, in the need of applying corrections during the data processing [1]. Requirements on the quality of the scan mirror drive can be relaxed by using optical compensation schemes [2,3], these can be as simple as the use of tilt-compensating retroreflectors like the cube corner [4] and the cat's eye [5,6]. If polarization distortions cannot be accepted, as in the polarizing interferometer according to the Martin–Puplett scheme [7], such retroreflectors are not suitable and more complex schemes involving foldings in the optical path are needed [8,9]. In the latter case, often only a partial optical compensation is obtained, and the mirror drive mechanism design is still a main issue, which requirements must be matched with the instrument optical design.

A system prototype of a parallelogram frictionless mirror drive and its application to a balloon-borne FTS, called REFIR (radiation explorer in

* Corresponding author. Tel.: +39 055 4378540; fax: +39 055 432694.
E-mail address: L.Palchetti@ifac.cnr.it (L. Palchetti).

1350-4495/$ - see front matter
doi:10.1016/j.infrared.2005.09.002

the far infrared) [10–12], and aimed to the study of the Earth's atmosphere spectral radiance in the 100–1100 cm^{-1} range, are presented in this paper. A description and the characterization of the realized prototype are reported in Sections 2 and 3, respectively. The performances on the balloon-borne instrument are also shown.

2. System description

The parallelogram mirror drive here described is designed for the REFIR prototype. The optical setup of the REFIR interferometer is depicted in Fig. 1 and it is described with many details in Ref. [3]. It is a Martin–Puplett scheme modified for using both planes of polarization of the input radiation. The input ports I_1, I_2 are located on the bottom instrument level, whereas the output ports O_1, O_2 are on the upper level. The two levels are separated inside the moving arms of the interferometer by using as retroreflectors two roof-top mirrors moving in a single unit (RTMU). In this way a folding of the optical path on two overlapped planes and a factor of 4 multiplier between mechanical scan and optical path difference (OPD) are obtained. $P(0°)$ and $P(45°)$ are 0° and 45° polarizing wire-grids, respectively. Input/output optics, and detector and calibration units are not reported in Fig. 1. The instrument uses one room-temperature pyroelectric detector per each output port in the focal plane of an off-axis parabolic mirror, and the calibration is performed by using two black-body reference sources.

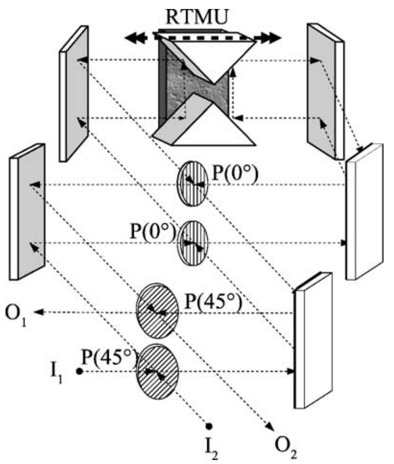

Fig. 1. Optical setup of the REFIR interferometer. I, O—input and output ports, P—polarizing beam splitters (with polarization angle), RTMU—roof-top mirror unit.

This configuration provides good performances over the whole REFIR spectral bandwidth and in particular the optical design provides some compensations of misalignment errors of the moving RTMU: because of the different number of reflections in the two arms, RTMU yaw affects in the same way both interfering wavefronts. RTMU pitch is compensated by the use of 90° roof-top mirrors. Both compensations operate in a first order approximation, and scan accuracy still depends on mirror drive. The mirror drive mechanism chosen for this application is shown in Fig. 2: a double parallelogram system supports the RTMU on one side, while on the other side is placed the scan motor. In principle, with this mechanism, RTMU translates parallel to itself without tilt errors. The hinges of the parallelograms make use of flexure pivots (C-FLEX, mod. E-10), that for the low deflection angles involved in the design, give an optimal solution to avoid friction and limit mechanism wear [13–15].

The maximum travel of the RTMU is about 12 mm, considering a parallelogram arm length of 58 mm, this translates into a maximum deformation of the flexure pivots of less than ±6°, well inside the factory specification of ±15° as maximum deformation for indefinite operating life. Considering the factor of 4 multiplier, the corresponding maximum path difference provides a spectroscopic resolution better than 0.2 cm^{-1} with double-sided interferogram acquisition. It should be noted that all the mechanical parts of the parallelogram mirror drive

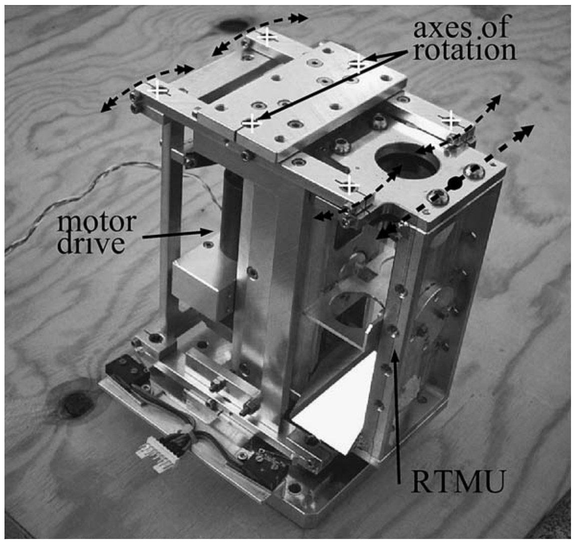

Fig. 2. Double parallelogram scan mirror drive with flexure pivot hinges (white +) and stepper motor drive.

are machined with a relaxed construction tolerance of about 0.1 mm.

The transmission providing linear motion of the parallelogram edge is another critical system: for the balloon prototype a simple and cost-effective solution was used, with a computer driven stepper motor (PI instruments, mod. Intellistep C-161.2i), a 100:1 reduction stage and a transmission based on a gear driving a toothed sector. The gear is coated with elastic material to damp motor vibrations and compensate for backlash. The driving gear diameter is 10.5 mm, the motor resolution is 20000 microsteps/turn, thus giving an OPD resolution of about 66 nm/microstep, enough to perform interferogram sampling up to visible wavelength even in presence of some amount of mirror drive granularity due to microstepping. While this solution is effective for the balloon application, involving operation times of the order of several hours, in prevision of a spaceborne application, a more suitable solution would be provided by a brushless linear motor with optical encoder.

The drive is operated in rapidly scanning mode and the position is controlled by counting the motor steps. Limit switches are used in order to define the starting position and to prevent possible overshoots. The chosen sampling approach, called "equal-time sampling with digital filter and numerical resampling", follows the method introduced by Brault [16] and is described in more details for application to the REFIR case in Ref. [17]. Interferograms are acquired with equal-time sampling together a reference signal, provided by a reference laser interferometer. From equal-time acquisition of both signals we obtain the equal-space interferogram for Fourier transformation.

3. Performance characterization

The performances of the mirror drive in terms of angular stability throughout the whole scan range are characterized by using both a collimated laser beam and a Zygo interferometer. First a rough estimate of the angular deviation was obtained by means of a laser beam reflected by a plane mirror placed on the RTMU. Angular deflection of the reflected beam has been estimated through a CCD sensor in the focal plane of a $f = 400$ mm lens. Subsequently, interferograms of the plane mirror have been acquired through the Zygo interferometer during a stepped scan. Analyzing the interference fringes an accurate estimate of angular deviation of the RTMU during scan has been obtained. The results of these two methods are shown in Fig. 3, and are in good agreement. Maximum angular deviation of about ± 0.4 mrad in the horizontal plane and ± 0.2 mrad in the vertical plane are measured.

The angular stability of the mirror drive can be used to calculate the effect of tilt errors on the interferometric efficiency in the case of the REFIR instrument. As already seen in Section 2, the peculiar optical scheme of this interferometer allows

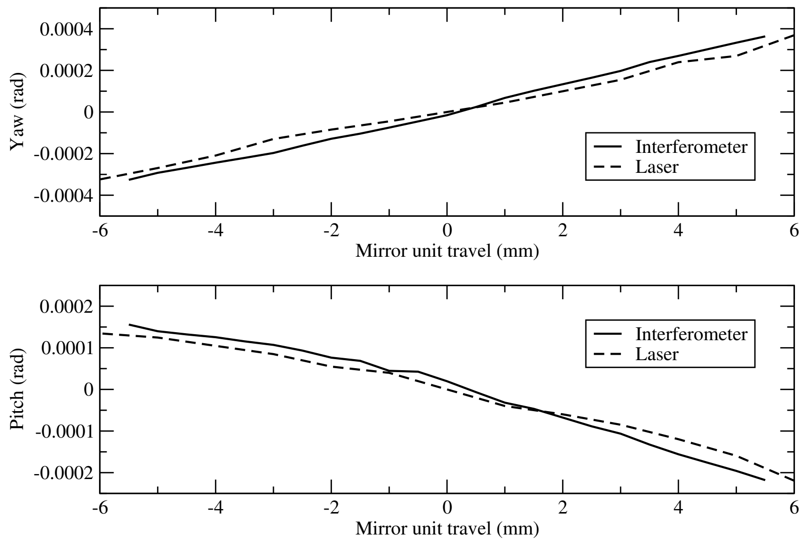

Fig. 3. Mirror unit deflection during scan measured with two independent methods (an interferometer and a laser beam with a position sensitive detector).

the compensation for tilt errors of RTMU. However the pitch error of RTMU produces a residual vertical shift of the beams, which is not fully compensated. This effect has been evaluated for the particular geometry of the REFIR interferometer. The resulting modulation efficiency is shown in Fig. 4 as a function of vertical tilt error of RTMU for different values of optical frequencies. The effect is a different apodization function depending on the optical frequencies. For frequency up to 500 cm^{-1} the apodization is practically negligible. The losses become relevant for frequencies above 1000 cm^{-1}. We notice however that if we take a spectral resolution equal to 0.5 cm^{-1}, as in the case of REFIR, the

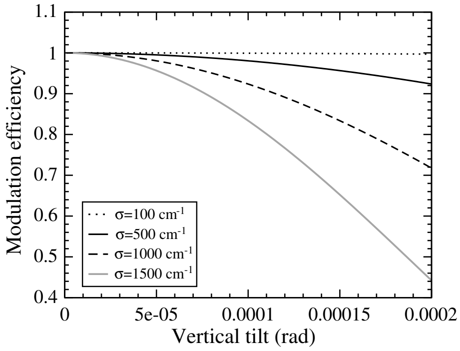

Fig. 4. Modulation efficiency of the interferometer as a function of RTMU vertical tilt calculated for different wavenumber values.

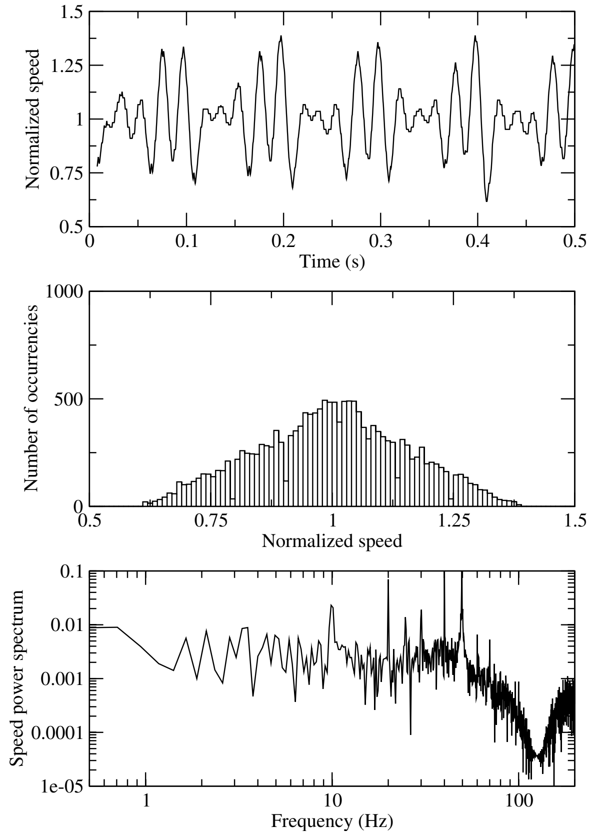

Fig. 6. Scan mirror speed characterization from fringe zero crossing count for the speed setting of 2000 microstep/s.

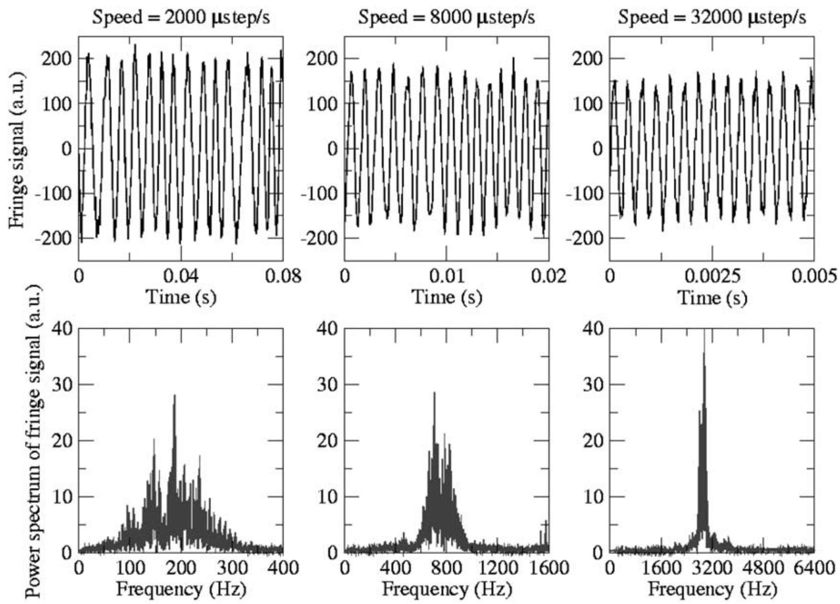

Fig. 5. Interference fringe frequency stability.

movement of RTMU can be limited to ±0.25 cm with a reduction of the pitch error to less than 0.1 mrad. As a consequence, the modulation efficiency results to be always above 80%.

While angular stability is the main requirement in the mirror drive, also an accurate speed control is needed to minimize sampling errors. In the adopted scheme involving a stepper motor, the main concern is motion granularity more than speed stability. Characterization of mirror motion has been obtained by using the reference laser interferometer.

An accurate characterization of speed stability of the mirror drive can be obtained from the frequency stability analysis of the laser fringes. In Fig. 5 we can see a sample of the laser fringes and the power spectrum of fringe signal for three different values of the speed, 2000, 8000 and 32 000 microsteps/s. The structure shown by the peak at the lower speed values indicates the presence of fringe modulation.

To further analyze and evaluate the amount of this effect, OPD vs. time has been calculated from fringe zero crossing count. In Figs. 6–8, upper panel, the normalized speed vs. time is shown for the three speed settings previously considered. An oscillating behavior is present at the lower speeds. The consequences of this effect on speed stability is clearly visible in the speed distribution histograms shown in Figs. 6–8, center panel. From the analysis of both the time series and the power spectrum of the normalized speed (Figs. 6–8 upper and lower panels), we notice that for each speed setting, an oscillation is present at a frequency proportional to the stepping frequency itself. At 2000 microsteps/s this oscillation occurs at 10 Hz, and gives rise to strong harmonics due to mechanical resonances in the system. At 8000 microsteps/s the forcing oscillation is at 40 Hz and fewer harmonics are present, while at the fastest speed setting (32 000 microsteps/s), the oscillation is greatly reduced being above all mechanical resonances, and the peak at 160 Hz is barely visible above noise.

The forcing oscillation identified in the speed spectrum can be interpreted as depending on the stepping motor. The driving stepper motor has a

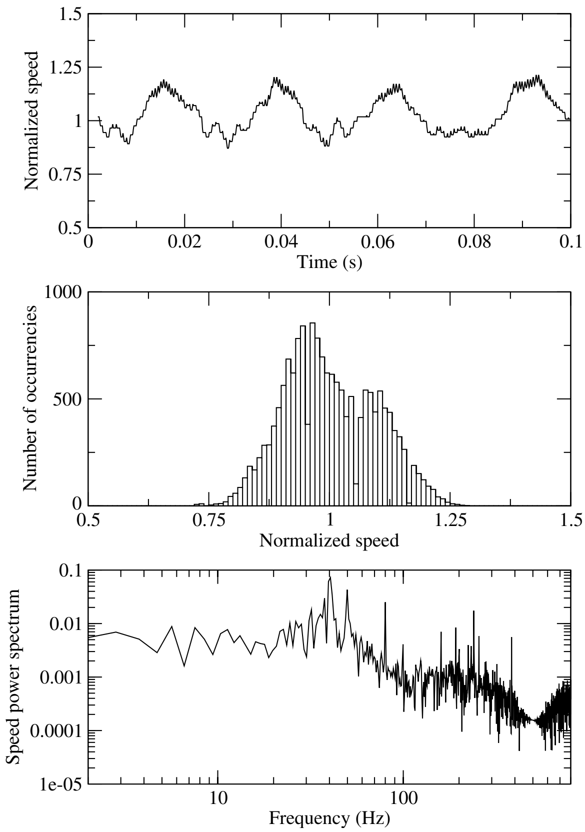

Fig. 7. Scan mirror speed characterization from fringe zero crossing count for the speed setting of 8000 microstep/s.

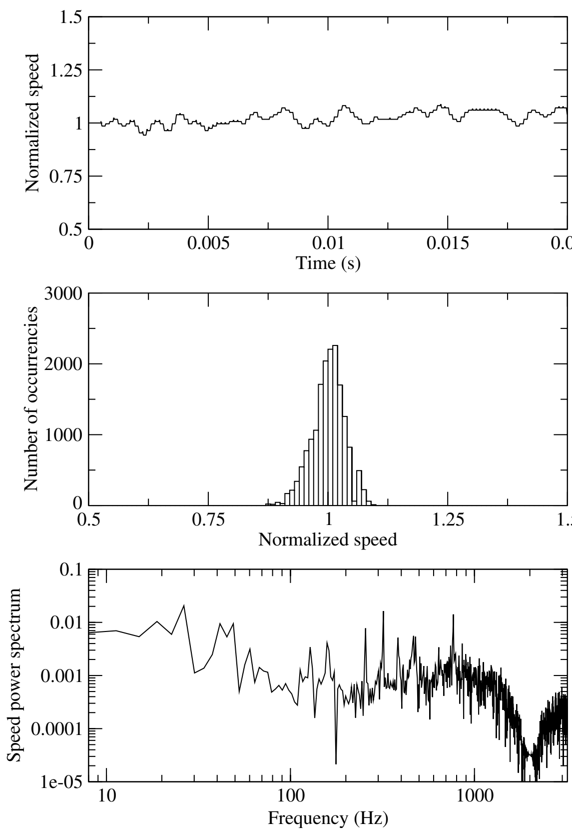

Fig. 8. Scan mirror speed characterization from fringe zero crossing count for the speed setting of 32 000 microstep/s.

native resolution of 400 steps/turn against an effective resolution of 20000 microsteps/turn.

The fluctuations in the mirror speed are reduced by the inertia of the mechanics when operating at high speed and, in any case, do not produce significant sampling errors if a proper sampling approach is used such as the equal-time sampling with digital filter and numerical resampling, mentioned above, used with the REFIR instrument. With this method it is shown that the spectral noise due to sampling error is reduced to about 1/2000 the signal with a rms speed error up to 7×10^{-5} m/s [17], which is greater than the peak value of 3×10^{-5} m/s measured in our drive.

While the deviation of less than 20% (worst case, i.e. lowest speed) is more than enough for the application, we clearly see how the use of a brushless DC motor with dedicated electronics can greatly improve speed stability characteristics of the mirror drive.

4. Conclusions

A simple, low-cost and compact mirror drive has been fabricated for Fourier transform spectrometer applications. The particular parallelogram mechanical structure with flexure pivots and the driving stepper motor have allowed good performances despite the relaxed accuracy required in the mechanical fabrication. An accuracy of 0.1 mm is sufficient for obtaining the performances shown in this paper in terms both of parallel translation, with tilt errors less than ±4 mrad. Also, the use of a simple stepper motor drive has provided enough speed accuracy, with errors less than 20% at the lowest speed and better than 5% at higher speeds. The low mechanical accuracy required in this design makes the system accessible at low-cost to any laboratory workshop facility. Neverthless, the relaxed requirements become acceptable for this critical part of an FTS instrument only when a comprehensive characterization, as shown in this paper, is made.

References

[1] G. Bianchini, P. Raspollini, Characterization of instrumental line shape distortions due to path difference dependent phase errors in a Fourier transform spectrometer, Infr. Phys. Tech. 41 (2000) 287–292.

[2] B. Carli, High-resolution far-infrared FT spectroscopy of the stratosphere: optimization of the optical design of the instrument, in: D.G. Cameron (Ed.), 7th International Conference on Fourier Transform Spectroscopy, Proceedings of SPIE, vol. 1145, 1989, pp. 93–98.

[3] B. Carli, A. Barbis, J.E. Harries, L. Palchetti, Design of an efficient broadband far-infrared Fourier-transform spectrometer, Appl. Opt. 38 (1999) 3945–3950.

[4] V. Formisano et al., PFS: a Fourier spectrometer for the study of Martian atmosphere, Adv. Space Res. 19 (1997) 1277–1280.

[5] L. Genzel, J. Kuhl, Tilt-compensated Michelson interferometer for Fourier transform spectroscopy, Appl. Opt. 17 (1978) 3304–3308.

[6] I.R. Abel, B.R. Reynolds, J.B. Breckinridge, J. Pritchard, Optical design of the ATMOS Fourier transform spectrometer, in: P.R. Yoder (Ed.), Optical System Engineering, Proceedings of SPIE, vol. 193, 1979, pp. 12–26.

[7] D.H. Martin, E. Puplett, Polarized interferometric spectrometry for the millimetre and submillimetre spectrum, Infr. Phys. 10 (1969) 105–109.

[8] B. Carli, P.A.R. Ade, U. Cortesi, P. Dickinson, M. Epifani, F.C. Gannaway, A. Gignoli, C. Keim, C. Lee, J. Leotin, F. Mencaraglia, A.G. Murray, I.G. Nolt, M. Ridolfi, SAFIRE/A—Spectroscopy of the atmosphere using far-infrared emission/airborne, J. Atm. Oceanic Tech. 16 (1999) 1313–1328.

[9] G. Bianchini, U. Cortesi, L. Palchetti, E. Pascale, SAFIRE/A (spectroscopy of the atmosphere by far-infrared emission—Airborne): optimised instrument configuration and new assessment of improved performances, Appl. Opt. 43 (2004) 2962–2977.

[10] REFIR—Radiation Explorer in the Far InfraRed, Final Report ENV4-CT6-0344, European Commission, Brussels, Belgium, 2000.

[11] L. Palchetti, A. Barbis, J.E. Harries, D. Lastrucci, Design and mathematical modelling of the space-borne far-infrared Fourier transform spectrometer for REFIR experiment, Infr. Phys. Tech. 40 (1999) 367–377.

[12] L. Palchetti, G. Bianchini, F. Castagnoli, B. Carli, C. Serio, F. Esposito, V. Cuomo, R. Rizzi, T. Maestri, Breadboard of the Fourier transform spectrometer for the radiation explorer in the far infrared atmospheric mission, Appl. Opt. 44 (2005) 2870–2878.

[13] R.V. Jones, Some uses of elasticity in instrument design, J. Sci. Instrum. 39 (1962) 193–203.

[14] D. Baker, A. Steed, A.T. Stair Jr., Development of infrared interferometry for upper atmospheric emission studies, Appl. Opt. 20 (1981) 1734–1746.

[15] R.C. Robinson, R.J. Huppi, S.L. Folkman, Optimization of a criogenic mirror stage, in: J.B. Heaney, L.G. Burriesci, (Eds.), Cryogenic Optical Systems and Instruments IX, Proceedings of SPIE, vol. 4822, 2002, pp. 93–98.

[16] J.W. Brault, New approach to high-precision Fourier transform spectrometer design, Appl. Opt. 35 (1996) 2891–2896.

[17] L. Palchetti, D. Lastrucci, Spectral noise due to sampling error in Fourier transform spectroscopy, Appl. Opt. 40 (2001) 3235–3243.